Load Regime of a Ferromagnetic Current Stabilizer

Ikromjon Rakhmonov[1, 2, a)], Abdulhay Rasulov[1], Mirjalol Ruzinazarov[1]
Urxiya Turabekova [1], Shokhrukh Azimov[1]

[1] *Tashkent state technical university named after Islam Karimov, Tashkent, Uzbekistan*
[2] *Termiz State University of Engineering and Agrotechnology, Termez, Uzbekistan*

[a)] *Corresponding author: ruzinzarov88@bk.ru*

Abstract. This article investigates the operating modes of a ferromagnetic current stabilizer (FCS) used in the control circuits of magnetic amplifiers under various load conditions. The study analyzes stable operating regimes for resistive, resistive–inductive, and resistive–capacitive loads based on mathematical modeling. The magnetization characteristic of the ferromagnetic element is approximated using a power-law function, enabling an analytical expression of the stabilization process to be derived.

INTRODUCTION

The application of ferroresonant circuits in the control circuits of magnetic amplifiers as signal generators for establishing a stabilization mode of the main operating circuit leads to a significant increase in output power without a substantial growth in the mass-dimensional characteristics of the stabilizer. According to [1,5], the total installed capacity of the reactive elements of a ferromagnetic current stabilizer (FCS) exceeds the load power by more than four times, which limits their application in high-power systems. It is therefore proposed to employ such circuits in the control schemes of magnetic amplifiers where only low power levels are required. In this way, the electromagnetic stabilizing device under investigation combines the advantages of a ferroresonant circuit and a magnetic amplifier. This device represents two interconnected nonlinear circuits, one of which performs the function of the executive element, while the other acts as a sensitive control element [6-9]. The simplest controllable ferromagnetic element consists of a working winding and a bias (control) winding wound on a closed ferromagnetic core. The bias winding is used to control the operating mode of the working winding and is supplied from a direct-current source [10-14].

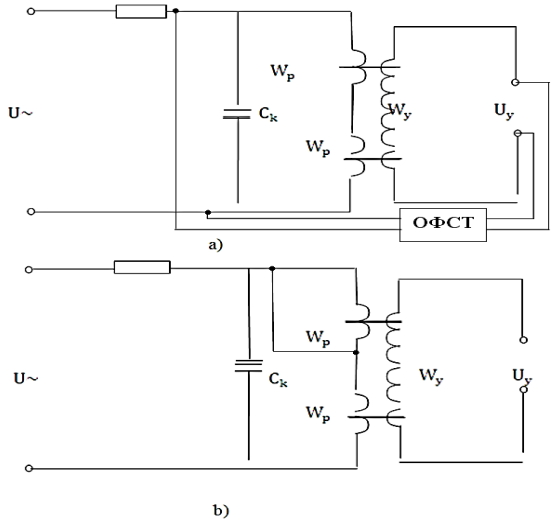

FIGURE 1. Circuit configurations of a ferromagnetic current stabilizer

EXPERIMENTAL RESEARCH

In order to determine the influence of various load parameters on the operation of a ferromagnetic current stabilizer and to evaluate its energy and operational characteristics, the load operating regime of the device is considered (Figure 1). Adopting the previously stated assumptions and neglecting losses in the magnetic amplifier, a steady-state analysis is performed for resistive, resistive–inductive, and resistive–capacitive loads.

$$u_c = R_H\left(i_c + i_{\text{фэ}}\right) + 2W_p\frac{d\phi}{dt}, \tag{1}$$

where u_c is the supply voltage, and $i_c$is the current flowing through the capacitor $C_к$

$$y = \delta\left(\frac{1}{m}\frac{d^2x}{d\tau^2} + i_{\text{фэ}}\right) + 2W_p\frac{d\phi}{dt} \tag{2}$$

Here,

$$\delta = \frac{R_H i_\delta}{2\omega W\phi_\delta}; m = \frac{i_\delta}{2\omega^2 W C_k\phi_\delta}; X = \frac{\phi}{\phi_\delta};$$

$$y = \frac{Uc}{U_\delta}; z = \frac{i}{i_\delta}; U_\delta = 2\omega W\Phi_\delta$$

Assuming that

$$y_m^2 = X_m^2 + \delta^2(Z_m - \frac{X_m}{m})^2 \tag{3}$$

$$tg\varphi = \frac{\delta(\frac{X_m}{m} - Z_m)}{X_m} \tag{4}$$

For further mathematical analysis, it is necessary to obtain an analytical expression for the characteristic X_m=f(Z_m). In this case, it is convenient to adopt an approximating function of the following form:

$$X_m = aZ_m^4 \tag{5}$$

Such a dependence qualitatively describes the characteristic of simultaneous magnetization in the operating region of the magnetic amplifier under stabilization conditions and provides sufficiently simple results for analyzing the load operating regime of the device [15-17]. The value of the coefficient depends on the magnitude of the bias current and can be determined using the method of selected points or the least squares method.

Substituting equation (5) into equation (3), we obtain:

$$y_m^2 = a^2Z_m^8 + \delta^2\left(Z_m - \frac{1}{m}aZ_m^4\right)^2 \tag{6}$$

Based on this expression, the control (regulation) characteristic of the current stabilizer can be constructed for various load resistances. The latter is characterized by the parameter δ, whose maximum admissible value is determined from the voltage–ampere characteristic (V–I curve) of the ferromagnetic current stabilizer circuit [18-22].

From the characteristic of the ferromagnetic current stabilizer circuit it can be seen that stabilization begins at (X_m=0,4) and continues up to (X_m=1,2). Thus, if we assume (y_m=1,2), the maximum voltage drop across the load should be determined by the following formula:

$$Y_{nm} = \sqrt{Y_m^2 + X_m^2}$$

Knowing the value of the stabilization current, we determine:

$$\delta = \frac{Y_{nm}}{Z_m} = 0{,}44; \qquad Z_m = 2{,}5$$

Thus, in the stabilization mode, variation of the parameter δ is allowed within the range from zero to 0.44. In this case, the input voltage must be equal to U=1.2 Figure 2 presents the regulation characteristics of the device for various values of active load resistance, constructed on the basis of equation (6).

For this case, the ratio of the installed capacity of the elements of the ferromagnetic current stabilizer to the load power is determined as follows:

$$q = \frac{\Sigma|Q|}{P_н} = \frac{|Q_{my}| + |Q_k|}{P_н} \tag{7}$$

Here, the maximum power of the magnetic amplifier, and the power of the compensating capacitor.

$$Q_{my} = Z_{my} * У_m; \qquad Z_{my} = 3{,}75; \qquad У_m = 1{,}2; \qquad Q_k = Z_{mk} * У_{mk}; \qquad Z_m = 1{,}2$$

From equation (7), we obtain that q≈2.

Thus, the installed capacity of the elements of the current stabilizer exceeds the load power by more than two times. This value is more than twice lower than that of the previously considered ferromagnetic current stabilizers (FCS).

For the case of a resistive–inductive load, the analysis is based on the following circuit equation:

$$u = R_н\left(i_c + i_{фэ}\right) + L\frac{d}{dt}\left(i_c + i_{фэ}\right) + 2W\frac{d\phi}{dt} \tag{8}$$

After performing simple transformations and introducing normalized variables, we obtain:

$$y = \delta(Z_c + Z_{фэ}) + \gamma_H \frac{d}{d_\tau}(Z_c + Z_{фэ}) + \frac{d_\phi}{d_\tau} \tag{9}$$

Here,

$$\delta = \frac{R_H i_\delta}{2\omega W \phi_\delta}; \quad \delta = \frac{L_H i_\delta}{2W\phi_\delta}: \quad Z_c = \frac{i_c}{i_\delta} \quad Z_{фэ} = \frac{i_{фэ}}{i_\delta}; \quad y = \frac{U}{U_\delta}: \quad U_\delta = 2\omega W \Phi_\delta$$

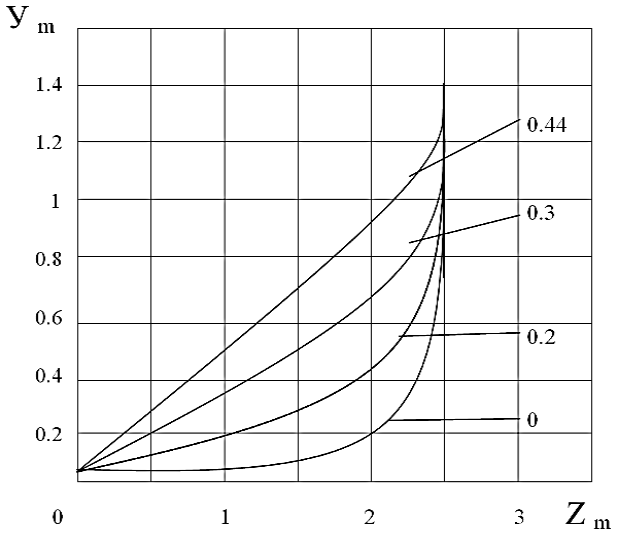

FIGURE 2. Regulation characteristics for a resistive (active) load

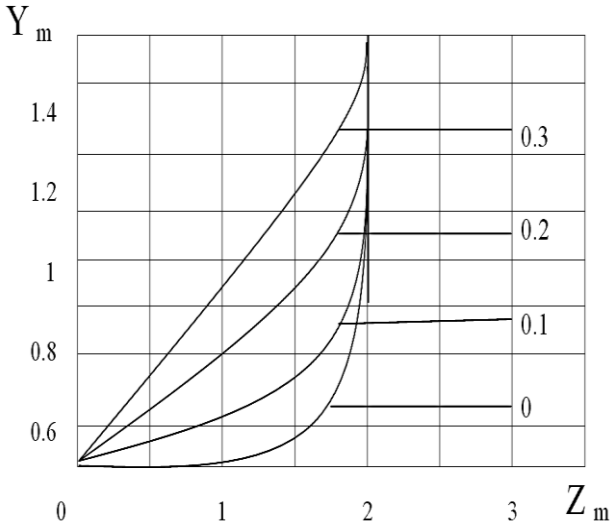

FIGURE 3. Regulation characteristics for a resistive–inductive load

$$Z_c = \frac{1}{m} \cdot \frac{d^2 \cdot x'}{d\tau^2}$$

$$y = Y_m \cos(\tau + \varphi) \tag{10}$$

$$x - X_m \sin \tau$$
$$z_{фэ} = Z_{mфэ} \sin \tau$$

If we adopt the approximating function of the simultaneous magnetization curve of the ferromagnetic element in the form given by equation (5), then after several transformations we obtain:

$$Y_m^2 = \delta^2 (Z_{mфэ} - \frac{aZ_{mфэ}^4}{m})^2 + \left[\gamma_H (Z_{mфэ} - \frac{aZ_{mфэ}^4}{m}) + aZ_{mфэ}^4 \right]^2 \tag{11}$$

Based on the latter dependence, taking into account that:

$$Z_{mcT} = Z_{mфэ} - \frac{Z_{mфэ}^4}{m},$$

Using this dependence, regulation characteristics of the current stabilizer can be constructed for various values of a resistive–inductive load (Fig. 3).

For a resistive–capacitive load, the circuit equation takes the following form:

$$. \frac{dU}{dt} = R_H \frac{d}{dt}(i_c + i_{фэ}) + \frac{i_c + i_{фэ}}{C_k} + W \frac{d^2 ф}{dt^2}$$

After a series of transformations, we obtain:

$$Y_m^2 = \delta^2 (Z_{mфэ} - \frac{aZ_{mфэ}^4}{m})^2 + \left[aZ_{mфэ}^2 - \gamma (Z_{mфэ} - \frac{aZ_{mфэ}^4}{m}) \right]^2 \tag{12}$$

CONCLUSION

The article presents a comprehensive analysis of the load operating modes of a ferromagnetic current stabilizer, with an in-depth study of its energy and operational characteristics. The research results show that a ferromagnetic current stabilizer applied in the control circuit of a magnetic amplifier has higher energy efficiency compared to conventional ferroresonant schemes. A comparative analysis of the regulation characteristics obtained for resistive, resistive–inductive, and resistive–capacitive loads revealed that the resistive–capacitive load is the most optimal option for current stabilization, since it provides a wider stabilization range. The results of the harmonic analysis indicate that the waveform of the stabilized current exhibits significant nonlinearity; therefore, the use of this stabilizer is most appropriate in control systems where strict requirements on current waveform are not imposed. Overall, the developed mathematical model and the graphical–analytical method are effective tools for the design and analysis of ferromagnetic current stabilizers and have important scientific and practical significance for applied power engineering devices.

REFERENCES

1. T. Kadyrov. Electromagnetic ferro-circuits possessing a wide descending region on the amplitude–phase characteristic. *Proceedings of Higher Educational Institutions. Electromechanics*, 1988, No. 7, pp. 26–30.
2. D. Jumaeva, B. Numonov, N. Raxmatullaeva, M. Shamuratova. Obtaining of highly energy-efficient activated carbons based on wood, // E3S Web of Conferences 410, 01018, (2023). https://doi.org/10.1051/e3sconf/202341001018

3. M. Taniev, M. Hamdamov, A. Sotiboldiev, Power Losses Of Asynchronous Generators Based On Renewable Energy Sources E3S Web of Conferences, 434, 01020, (2023) https://doi.org/10.1051/e3sconf/202343401020
4. O. Toirov, S. Khalikov, Sodikjon Khalikov, F. Sharopov, Studies of reliability indicators of pumping units of machine irrigation on the example of the "Namangan" pumping station, // E3S Web of Conferences 410, 05015, (2023). https://doi.org/10.1051/e3sconf/202341005015
5. M. Rosenblat. *Magnetic Amplifiers with Self-Saturation*. Moscow: State Energy Publishing House (GEI), 1963, 127 p.
6. A. Rasulov, M. Melikuziev. Methodology for calculating electromagnetic ferro-circuits using approximation of the magnetization curve by a generalized n-th order function. *International Scientific Review*, No. 4 (II).
7. O. Toirov, T. Kamalov, U. Mirkhonov, S. Urokov, D. Jumaeva, The mathematical model and a block diagram of a synchronous motor compressor unit with a system of automatic control of the excitation // E3S Web of Conferences, 288, 01083, (2021), https://doi.org/10.1051/e3sconf/202128801083
8. D. Bystrov, S. Giyasov, M. Taniev, S. Urokov. Role of Reengineering in Training of Specialists // ACM International Conference Proceeding Series (2020) https://doi.org/10.1145/3386723.3387868
9. V. Ivanova, V. Tsypkina, D. Jumaeva, D. Abdullaeva, Improvement of the multifilament wire lager for cable production, // E3S Web of Conferences 411, 01041 (2023), https://doi.org/10.1051/e3sconf/202341101041
10. O. Toirov, S. Urokov, U. Mirkhonov, H. Afrisal, D. Jumaeva, Experimental study of the control of operating modes of a plate feeder based on a frequency-controlled electric drive, // E3S Web of Conferences, SUSE-2021, 288, 01086 (2021). https://doi.org/10.1051/e3sconf/202128801086
11. S. Khalikov, Diagnostics of pumping units of pumping station of machine water lifting, // E3S Web of Conferences 365, 04013, (2023). https://doi.org/10.1051/e3sconf/202336504013
12. M. Khalikova, D. Jumaeva, S. Kakharov, (2023) Development of a mathematical model of a frequency-controlled electromagnetic vibration motor taking into account the nonlinear dependences of the characteristics of the elements, // E3S Web of Conferences 401, 05089, (2023). https://doi.org/10.1051/e3sconf/202340105089
13. O. Toirov, S. Khalikov. Analysis of the safety of D. Bystrov, M. Gulzoda, Y. Dilfuza, Fuzzy Systems for Computational Linguistics and Natural Language (2020) // ACM International Conference Proceeding Series, https://doi.org/10.1145/3386723.3387873
14. I. Khujaev, J. Jumayev, M. Hamdamov, Modeling of vertical axis wind turbine using Ansys Fluent package program, // E3S Web of Conferences 401, 04040 (2023). https://doi.org/10.1051/e3sconf/202340104040
15. D. Jumaeva, A. Abdurakhimov, Kh. Abdurakhimov, N. Rakhmatullaeva, Energy of adsorption of an adsorbent in solving environmental problems, // E3S Web of Conferences, SUSE-2021, 288, 01082 (2021). https://doi.org/10.1051/e3sconf/202128801082
16. O. Toirov, D. Jumaeva, U. Mirkhonov, S. Urokov, S. Ergashev, Frequency-controlled asynchronous electric drives and their energy parameters, // AIP Conference Proceedings 2552, 040021, (2022). https://doi.org/10.1063/5.0218808
17. A. Rasulov, R. Ruzinazarov. Ferroresonant devices for current stabilization. *Universum: Technical Sciences*, No. 3–4, pp. 5–9, 2016.
18. V. Bedritsky. DC current stabilizers with a controlled inductive element in a ferroresonant circuit. In: *Proceedings of the XI International Scientific Conference "Current Issues of Modern Engineering and Technology"*, April 14, 2014, Lipetsk, Russia, pp. 77–81.
19. O. Toirov, T. Sadullaev, D. Abdullaev, D. Jumaeva, Sh. Ergashev, I.B. Sapaev, Development of contactless switching devices for asynchronous machines in order to save energy and resources, // E3S Web of Conferences 383, 01029, (2023). https://doi.org/10.1051/e3sconf/202338301029
20. S. Khalikov, Algorithm and Software Implementation of the Diagnostic System for the Technical Condition of Powerful Units, // E3S Web of Conferences 377, 01004, (2023). https://doi.org/10.1051/e3sconf/202337701004
21. D. Jumaeva, Z. Okhunjanov, U. Raximov, R. Akhrorova. Investigation of the adsorption of nonpolar adsorbate molecules on the illite surface, // Journal of Chemical Technology and Metallurgy, 58, 2, (2023). https://doi.org/10.59957/jctm.v58i2.61
22. O. Toirov, K. Alimkhodjaev, A. Pardaboev, Analysis and ways of reducing electricity losses in the electric power systems of industrial enterprises, // E3S Web of Conferences, SUSE-2021, 288, 01085 (2021). https://doi.org/10.1051/e3sconf/202128801085